Probabilistic assessment of spatial heterogeneity of natural background concentrations in large-scale groundwater bodies through Functional Geostatistics

L. Guadagnini[a,*], A. Menafoglio[b], X. Sanchez-Vila[a], A. Guadagnini[c]

[a]Department of Civil and Environmental Engineering, Universitat Politècnica de Catalunya, Jordi Girona 1-3, 08034 Barcelona, Spain

[b]Politecnico di Milano, MOX, Department of Mathematics, Piazza L. Da Vinci 32, 20133 Milano, Italy

[c]Politecnico di Milano, Dipartimento di Ingegneria Civile e Ambientale, Piazza L. Da Vinci 32, 20133 Milano, Italy

*Corresponding author: laura.guadagnini@polimi.it, laura.guadagnini@upc.edu

Abstract

We propose and exemplify a framework to assess Natural Background Levels (NBLs) of target chemical species in large-scale groundwater bodies based on the context of Object Oriented Spatial Statistics. The approach enables one to fully exploit the richness of the information content embedded in the probability density function (PDF) of the variables of interest, as estimated from historical records of chemical observations. As such, the population of the entire distribution functions of NBL concentrations monitored across a network of monitoring boreholes across a given aquifer is considered as the object of the spatial analysis. Our approach starkly differs from previous studies which are mainly focused on the estimation of NBLs on the basis of the median or selected quantiles of chemical concentrations, thus resulting in information loss and limitations related to the need to invoke parametric assumptions to obtain further summary statistics in addition to those considered for the spatial analysis. Our work enables one to (*i*) assess spatial dependencies among observed PDFs of natural background concentrations, (*ii*) provide spatially distributed kriging predictions of NBLs, as well as (*iii*) yield a robust quantification of the ensuing uncertainty and probability of exceeding given threshold concentration values via stochastic simulation. We illustrate the approach by considering the (probabilistic) characterization of spatially variable NBLs of ammonium and arsenic detected at a monitoring network across a large scale confined groundwater body in Northern Italy.

Keywords: Natural background level; groundwater quality; chemical status; Kriging; probability density function; Uncertainty Quantification.

1. Introduction

Robust characterization of the natural chemical signature of a given groundwater system is a key component of modern environmental analysis. Critical aspects associated with this step include the identification of values of sampled concentrations of target chemicals that could be related to geogenic contributions. In this context, it is recognized that markedly high Natural Background levels (NBLs) of chemical species/compounds of interest can potentially be linked to petrographical (e.g., Hinsby and Condesso de Melo, 2006) or lithological and sedimentological site-specific characteristics (e.g., Redman et al., 2002; Molinari et al., 2013 and references therein) rather than being attributable to anthropogenic actions. Relating high values of sampled concentrations to an anthropogenic rather than a natural contribution may sometimes yield misleading assessments of environmental risks, improper classification of the chemical status (e.g., in terms of a good status, as defined by the European Water Framework Directive, WFD 2000/60/EC GWDD 2006/118/EC Directive 2014/80/EU) of aquifer bodies, as well as setting remediation goals which can be unattainable and/or unsustainable. In this context, modern regulatory frameworks at the European level highlight the need for an appropriate assessment of baseline concentrations, i.e. those that can be ascribed to geogenic effects and not caused by anthropogenic activities.

Identification and implementation of a complete (generally multicomponent) geochemical model accounting for the complexity of processes driving flow and transport in porous media in the presence of the various sources of uncertainty associated with the ubiquitously heterogeneous subsurface is not always feasible. A series of investigations are then keyed to the development of procedures leading to embedding information within a management framework upon relying on a limited amount of data. The latter typically comprise monitored temporal series of concentration samples (Edmunds et al., 2003, Wendland et al., 2005, Panno et al., 2006, Walter, 2008, Urresti-Estala et al., 2013, Kim et al., 2015; Liang et al., 2017, 2018, 2019).

As an example, one of the main outcomes of the EU funded project BRIDGE (2007), Background cRiteria for the IDentification of Groundwater thrEsholds, is a guideline that allows

64 assessing the natural status of a groundwater body through a Pre-Selection methodology. The latter
65 is based on the identification of pristine groundwater samples within an available collection of
66 observations. This procedure typically yields the estimate of a unique (or bulk) NBL value, which is
67 then assigned to the groundwater body under investigation. According to this approach,
68 concentration values of a chemical species of interest exceeding such a threshold are then ascribed
69 to anthropogenic activities. A notably weak point of such an approach is that it renders a unique
70 NBL value, disregarding spatial variability, this aspect being critical when considering large scale
71 heterogeneous (in terms of petrographic and hydrogeologic characteristics) aquifers. As a further
72 evolution, some authors suggest that the NBL of a natural groundwater system should be expressed
73 in terms of a range of values (e.g., Reimann and Garrett, 2005; Hinsby et al., 2008; Li et al., 2014)
74 rather than being constrained to a single one.
75 Studies related to characterizing the spatial variability of NBL concentrations include, e.g.,
76 the work of Ducci et al. (2016) and Dalla Libera et al. (2017). While the former relies on indicator
77 kriging to demarcate regions associated with given probability of exceeding a target NBL value, the
78 latter authors propose a zonation approach leading to piece-wise uniform NBL concentration maps.
79 The analysis of Molinari et al. (2019) starts from values of the 90^{th} percentile of concentration
80 samples observed at a set of monitoring boreholes. These are then subject to standard variography
81 upon considering alternative variogram models which are then employed in a multimodel context to
82 provide kriging-based spatial distributions of estimates of NBL concentrations. The resulting kriged
83 values are used jointly with the ensuing estimation variance to evaluate spatial distributions of the
84 probability of exceeding predefined threshold values of NBL concentrations, the latter being
85 assumed to be characterized by a log-normal distribution. We emphasize that all of these works rely
86 on the representation of observed temporal series of natural background concentrations by way of
87 through scalar summaries (e.g., the 90^{th} percentile), which are then projected onto a set of locations
88 of interest where data are not available. Doing so results in a loss of information and requires
89 resorting to additional hypothesis, such as assuming a log-normal distribution for NBL values

90 which is parametrized according to the results of the kriging analysis (as in, e.g., Molinari et al.,
91 2019). The general concept underlying these studies is also consistent with approaches treating the
92 characterization of spatial heterogeneity of aquifer systems within a probabilistic context (e.g.,
93 Winter et al., 2003; Short et al., 2010; Perulero Serrano et al., 2014; Bianchi Janetti et al., 2019 and
94 references therein).

95 Our study rests on the concepts underpinning Object Oriented Data Analysis (Marron and
96 Alonso, 2014). Doing so enables us to consider the information content included in the entire
97 distribution function of NBL concentrations monitored at a given observation borehole as the object
98 of the spatial analysis, instead of being limited to selected moments or quantiles. Such a framework
99 renders (*a*) predictions of the complete distribution of NBL concentrations in a non-parametric
100 setting together with the associated uncertainty, and (*b*) joint assessment of all summary quantities
101 of interest of the distribution (including desired quantiles and probability values). Accordingly, the
102 NBL distributions are embedded in a mathematical space whose elements are probability density
103 functions (Egozcue et al., 2006, Van den Boogaart et al., 2014). Our distinctive objective is to
104 leverage on key elements of Object Oriented Spatial Statistics (O2S2, Menafoglio and Secchi,
105 2017) to (*i*) quantify spatial dependencies among observations, (*ii*) provide spatially distributed
106 kriging predictions, and (*iii*) yield a robust quantification of the uncertainty associated with NBL
107 spatial distributions through stochastic simulation. As detailed in the following, we first illustrate
108 the theoretical framework, and then demonstrate it to characterize spatial variability of NBL
109 distributions of target chemical species by relying on an extensive set of hydrochemical data
110 collected across a large scale confined groundwater body in Northern Italy.

111 ## 2. Materials and methods

112 ### *2.1. Study area and data-set*

113 As a test bed to demonstrate the breadth and potential of our approach, we focus on a
114 groundwater body located in the Emilia-Romagna Region (Northern Italy) and demarcated on the
115 basis of both geological/sedimentological information and anthropogenic impact analyses (Regione

Emilia-Romagna, 2010). The area is a portion of the Po Basin fill, a syntectonic sedimentary wedge (Ricci Lucchi, 1984) forming the infill of the Pliocene-Pleistocene fore-deep.

Sedimentological and hydrogeological studies are available in the region (Amorosi et al., 1996; Regione Emilia-Romagna-ENI-AGIP, 1998, Regione Emilia-Romagna, 2010), identifying three main hydrogeological complexes: Apennines alluvial fans, Apennine alluvial plain, and alluvial and deltaic Po plain. The complete aquifer system is characterized by a multilayered confined or semiconfined configuration. The thickness of fine deposits increases towards the northern portion of the plain (Regione Emilia-Romagna, 2010; Farina et al., 2014), where conditions of increased confinement are documented.

Additional information regarding the hydrogeological setting of the region are available in Molinari et al. (2012) and Farina et al. (2014). Our study is keyed to one of the large scale groundwater bodies located in the upper confined portion of the aquifer system, within the hydrogeological complex named as Appenine alluvial plain. Figure 1 depicts limits and planar extent of the groundwater body considered, denoted with the identifier 0610 and characterized by an average depth of 75 m, average thickness of 130 m and area of about 2930 km^2.

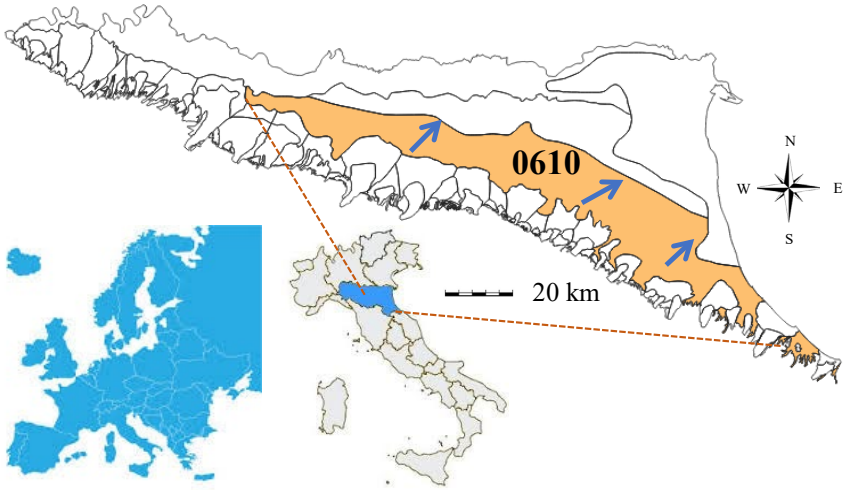

Figure 1. Planar extent of groundwater body 0610 within the Emilia-Romagna Region. Blue arrows correspond to the overall regional-scale groundwater flow direction.

The groundwater body under study is considered to be significantly vulnerable, given its stratigraphic location within the aquifer system and the anthropogenic stresses associated with intensive exploitation for agricultural and civil purposes (Regione Emilia-Romagna, 2010). Being located in the upper confined portion of the complex aquifer system described, its southern limit is in continuity with the recharging areas of alluvial fans. A relevant amount of monitoring boreholes is set within its considerable planar extent, thus yielding a remarkable amount of available chemical data. As evidenced in prior investigations (Molinari et al. 2012, 2019), data about groundwater quality suggest the need to considering regional-scale, spatially heterogeneous distributions of NBL values.

The analyzed data set includes time series of concentrations recorded at several monitoring stations managed by the "Agenzia Regionale per la Prevenzione e l'Ambiente dell'Emilia-Romagna" (ARPAE - Regional Agency for Environmental Protection, Emilia-Romagna). We select monitoring boreholes where 20-year historical records of observations (1987-2008, collected at a six-month interval, albeit not continuously for some wells) are available. We focus on ammonium (NH_4) and arsenic (As), whose documented concentrations locally exceed the limit set by current Italian regulations (also corresponding to the European Drinking Water Standards) set at 0.5 mg/l and 10 µg/l, respectively, and are seen as critical elements for the achievement of a good chemical status according to Italian Regulation (D. Lgs. 30/09, i.e., Decreto Legislativo n. 30, 16 March 2009) and GWDD 2006/118/EC. A total number of 90 monitoring stations was initially considered by ARPAE to characterize groundwater body 0610. Some of these were associated solely with quantitative measurements of piezometric level. On the basis of a subsequent detailed analysis, monitoring stations that could not be attributed with certainty to the target groundwater body (essentially on the basis of the screen depth) were excluded from the original collection of locations. This has reduced the initial number of monitoring stations attributed to groundwater body 0610 to 62, with a total of 1428 observations. Exclusion of monitoring stations where observations are associated with a temporal window spanning less than 3 years leads to retain 57 monitoring stations

with a total of 1354 observations available (among these, ammonium and arsenic have been measured in 1343 and 1193 samples, respectively). Concentrations below detection limit were set equal to half the detection limit. After application of PS, monitoring stations where less than 10 data points are available are further excluded from our analyses. As such, we use 1234 (associated with 44 monitoring stations) for ammonium (see Section 3.1) and 1096 data (related to 43 monitoring stations) for arsenic (see Section 3.2).

2.3 Methodology for Data analysis

2.3.1 NBL estimates

Concentration records are subject to a Pre-Selection (PS) procedure (BRIDGE, 2007) to identify NBL values. This approach enables us to remove samples exceeding certain concentration values, considered indicative of anthropogenic contamination, from the original record of observations. Conditions for samples exclusion are: (*a*) chloride concentrations > 1000 mg/l, denoting salinity; and (*b*) nitrate (NO_3) concentrations > 10 mg/l, as a signature of anthropogenic influence caused by e.g., fertilizers. Additional criteria (redox conditions, dissolved oxygen, sulfate concentration) can be considered for sample exclusion (e.g., Hinsby and Condesso de Melo, 2006; Hinsby et al., 2008). For the purpose of our analyses, we follow Molinari et al. (2019) and apply only the exclusion criteria listed above.

Data resulting from filtering the raw dataset through PS are considered as observations of naturally occurring NBL concentrations at diverse observation times across the analyzed window. Our analysis rests on monitoring wells which exhibit a time series with more than ten records. We note that the procedure which is then employed for the evaluation of the NBL (e.g., Wendland et al., 2005) relies on (*a*) estimating the median value for the concentrations of the target chemical species identified at each monitoring well via PS, and (*b*) assessing the unique value of NBL associated with the whole water body in terms of a selected percentile (typically the 90^{th}, 95^{th}, or 97.5^{th}).

As illustrated in details in Section 2.3.3, we adopt here a diverse perspective and fully account for the functional nature of the data. The latter are thus analyzed as functional random

fields. In this context, the subject of our analysis is the collection of probability functions of NBLs obtained by applying the PS procedure at each monitoring station. By doing so, we go beyond the limitation of relying solely on selected percentiles of such probability functions and take advantage of the complete information content embedded in the entire probability function of NBL reconstructed from the observations at each well.

We structure our study through the following main steps:

1. perform sample selection for historical records at each observation borehole following the adopted exclusion criteria, as indicated in the original BRIDGE (2007) methodology;
2. evaluate the (empirical probability) distribution function of NBLs of (log-transformed) concentrations of the selected chemical species at each observation well;
3. perform spatial prediction and uncertainty quantification of NBL probability density functions (PDFs) at unsampled locations using an object-oriented geostatistical approach (Menafoglio et al., 2014).

We describe the main theoretical elements and the ensuing implementation workflow associated with these steps in the following sections.

2.3.2 Data pre-processing

Data pre-processing aims at extracting an estimate of the NBL PDFs from each temporal series of NBL observations. Each temporal series is considered separately (observations associated with the series being used to build a corresponding histogram) neglecting temporal autocorrelation (additional comments on this choice are given in Section 3). The resulting histogram is then smoothed to yield a continuous estimate of the underlying PDF, as advocated by Machalová et al. (2016) and consistent with the modeling framework employed for the following analysis steps (detailed in Sections 2.3.3-2.3.4). Note that the length of the time-series can have an effect on the accuracy of the PDF estimation, i.e., the longer the time series, the lower the uncertainty in the data-preprocessing. Here, we include all monitoring stations where at least 10 records are available. This is seen as a minimum threshold value to maintain the ability of estimating a density function from

the sampled data with a non-parametric approach. In general, the choice of such a threshold should attain a balance between the ability of estimating the PDF with sufficient accuracy, and the need to retain as many measurement sites as possible. This choice is case-specific and depends on the stability of the time-series, the data quality, possible missing data, the density of the measurement locations and their spatial distribution.

2.3.3 Notation and background: geostatistics for PDFs

The smoothed PDF data are considered as the objects of the geostatistical analysis. In the following we denote by $s_1, \dots, s_n$ the n locations in the spatial domain D where the PDFs of NBL are observed, and by $X_{s_1}, \dots, X_{s_n}$ the n smoothed PDFs available at the sampling locations. Here, X_{s_i} denotes the PDF at location s_i, which is a positive function defined on an interval of (log-)concentrations $I = [a, b]$, common to all data. We consider these PDFs as a partial observation of a *functional* random field $\{X_s, s \in D\}$, that is a collection of random functional elements (the PDFs of NBL) indexed by a spatial variable s in D. The goal of the analysis is to provide a kriging prediction of the random field (i.e, the entire PDF, X_{s_0}) at unsampled locations (s_0) in D, based on the observations available at the monitoring stations. Two key challenges need to be tackled to solve the kriging problem: (*i*) the curse of dimensionality (due to the virtually infinite dimensionality of PDF data, which would need an infinity of point evaluations to be fully characterized), and (*ii*) the data constraints (positivity and unit integral).

To jointly face these challenges, we follow the approach of Menafoglio et al. (2014, 2016a, 2016b), who provide a class of geostatistical methods to analyze datasets of geo-referenced PDFs. These methods are based on the idea of defining an appropriate mathematical space where data are embedded, and use the geometry of the space to perform prediction and stochastic simulation. For instance, if the NBL data were represented through their median (i.e., a scalar summary statistics), the data could be embedded in the space R of real numbers, and analyzed through a typical scalar geostatistics approach. If the NBL data were represented through a set of k summary indices (e.g.,

mean and standard deviation), a k-dimensional Euclidean space R^k could be used to perform analyses through multivariate geostatistical methods (e.g., Chilès and Delfiner, 1999). Considering functional and constrained data, Menafoglio et al. (2014, 2016a, 2016b) propose to consider a Bayes space (Egozcue et al., 2006; Van den Boogaart et al., 2014), whose elements are PDFs, for embedding and analyzing the data. Bayes spaces provide the generalization to the functional framework of the so-called Aitchison simplex (Aitchison, 1986). In Bayes spaces, appropriate notions of operations between PDFs (e.g., sum $(+)$, or product by a constant $(\cdot)$) as well as of inner product $(\langle\cdot,\cdot\rangle)$ are defined, allowing for the development of a proper theory of kriging and stochastic simulation. For the purpose of this study, we do not present all details of these mathematical constructions and introduce only the key concepts and notation. We refer to Menafoglio et al. (2013, 2014, 2016a, 2016b) for an in-depth introduction to the mathematics underpinning the methods we employ.

2.3.4 Modeling spatial dependence and kriging

As a first step of the geostatistical analysis of the dataset $X_{s_1}, \dots, X_{s_n}$ of PDFs, we model the spatial dependence among data. We assume that (*a*) data are elements of the Bayes space B^2, that is the space of positive functions, whose natural logarithm is square integrable, and (*b*) the field $\{X_s, s \in D\}$ is stationary. This enables us to consider the generalization of the classical variogram to the functional context, which is termed *trace-variogram*. In B^2, the trace-variogram is defined as the function $2\gamma(s_1, s_2)$ that associates with a pair of locations s_1, s_2 (in D) the expected square distance (in B^2) between the NBL PDFs (X_{s_1}, X_{s_2}) at such locations, i.e.,

$$2\gamma(s_1, s_2) = \mathbb{E}\left[d_{B^2}^2\left(X_{s_1}, X_{s_2}\right)\right] = \mathbb{E}\left[\frac{1}{2(b-a)}\int_a^b\int_a^b \ln\left(\frac{X_{s_1}(t)X_{s_2}(s)}{X_{s_1}(s)X_{s_2}(t)}\right)dtds\right]. \quad (1)$$

Interpretation and properties of the trace-variogram for PDF data are very similar to their scalar counterpart. In particular, under stationarity, the trace-variogram depends only on the increment among locations $(s_1 - s_2)$, stabilizes at a horizontal asymptote (*sill*), and the distance at which the variogram attains the sill determines the range of association among elements of the field (*range*).

263 Variogram modeling can be performed in two steps: (*i*) estimating a binned trace-variogram

264 $$2\gamma(h) = \frac{1}{|N(h)|}\sum_{s_i,s_j \in N(h)} d^2_{B^2}\left(X_{s_i}, X_{s_j}\right), \quad (2)$$

265 $|N(h)|$ being the number of pairs of sampled sites (approximately) separated by h; and (*ii*) fitting a
266 valid model (e.g., spherical, exponential, matérn) to the empirical estimate (1).

267 Once the variogram model is estimated, the *functional* kriging prediction for a PDF of NBL at
268 a target location s_0 is based on the best linear unbiased (functional) predictor in the Bayes space B^2.
269 This is defined as the predictor $X^*_{s_0} = \sum_{i=1}^n \lambda_i^* \cdot X_{s_i}$, where symbols denote the linear combination in
270 the Bayes space, and are explicitly written as

271 $$X^*_{s_0}(t) = \frac{\prod_{i=1}^n X_{s_i}^{\lambda_i^*}(t)}{\int_a^b \prod_{i=1}^n X_{s_i}^{\lambda_i^*}(s)ds}, \quad (3)$$

272 $\lambda_1^*, \dots, \lambda_n^*$ being scalar weights to be optimized through minimization of the variance of prediction
273 error under unbiasedness. From a practical viewpoint, having estimated the trace-variogram model
274 2γ, finding the kriging weights reduces to the solution of the very same kriging system associated
275 with scalar geostatistics (see, e.g., Menafoglio and Secchi, 2017, for details).

276 *2.3.5 Stochastic Simulation*

277 Uncertainty quantification for functional kriging can be performed by using conditional
278 stochastic simulation, as originally proposed in Menafoglio et al. (2016b). For this purpose, one
279 necessarily needs to reduce the dimensionality of the data, as it is hardly possible to produce
280 realizations of an infinity of point evaluations of the PDF. Dimensionality reduction can be
281 performed through functional principal component analysis in the Bayes space B^2 (SFPCA, Hron et
282 al., 2016). The SFPCA analysis allows identifying the main directions of variability $(e_1, e_2, \dots)$ of
283 the dataset $X_{s_1}, \dots, X_{s_n}$. The elements $e_1, e_2, \dots$ are the analogue of the eigenvectors in multivariate
284 principal component analysis. In particular, $e_1, e_2, \dots$ form an orthonormal functional basis of space
285 B^2. Projecting the data along the first K principal components enables one to represent the PDF X_{s_i}
286 through a vector of K coordinates $\boldsymbol{x}_{s_i} = (x_{s_i,1}, \dots, x_{s_i,K})$, thus reducing to K the formerly infinite

dimensionality of the PDF. Stochastic simulation of the PDF can be then performed by simulation of the vector of coordinates along the truncated basis $e_1, e_2, \dots, e_K$ at the target location $\boldsymbol{x}_{s_0} = (x_{s_0,1}, \dots, x_{s_0,K})$, based on the coordinate vector available at the sampled sites. Such simulation can be performed through the aid of well-known multivariate methods, such as those based on sequential Gaussian co-simulation (e.g., Chilès and Delfiner, 1999; Kim et al., 2019).

3. Results and discussion

3.1. Ammonium

As stated in Section 2.1, a total of 1234 historical records collected at 44 monitoring stations were available for ammonium concentration after PS, characterized by a number of 12 to 42 observations per monitoring well (with an average of about 28). A preliminary analysis of the data reveals that most locations (41 out of 44) do not display any autocorrelation in the time series of NBL concentrations (level 1%, as obtained through a Durbin-Watson test on each time series, the p-value of single tests being corrected via Holm's method). Autocorrelation within the temporal series was thus neglected in the data preprocessing. The PDF of NBL log-concentrations (hereafter termed NBL densities or NBL PDFs for ease of illustration) were then estimated at each borehole upon neglecting temporal autocorrelations. The ensuing results are depicted in Figure 2 in terms of smoothed data.

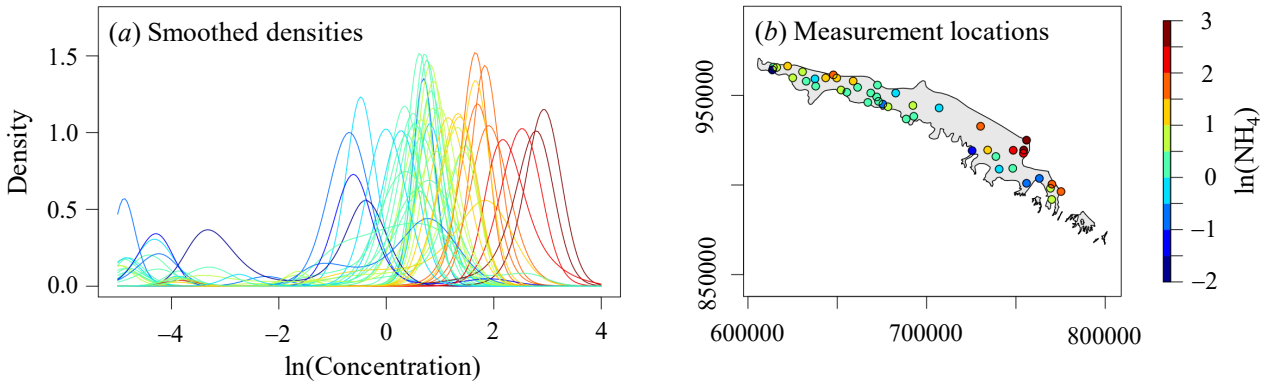

Figure 2. Smoothed data for ammonium log-concentration values and corresponding spatial locations in the investigated aquifer system. Colors are assigned according to the value of the mean related to the corresponding smoothed density. Spatial coordinates are in meters.

Visual inspection of Figure 2 suggests that the highest mean values are associated with the distal portion of the domain, mainly close to the coastal area where water is characterized by high chloride concentrations. A global stationarity assumption of the functional data appears to be supported by the sample trace-semivariogram depicted in Figure 3, which is characterized by a clear asymptote for increasing spatial distances.

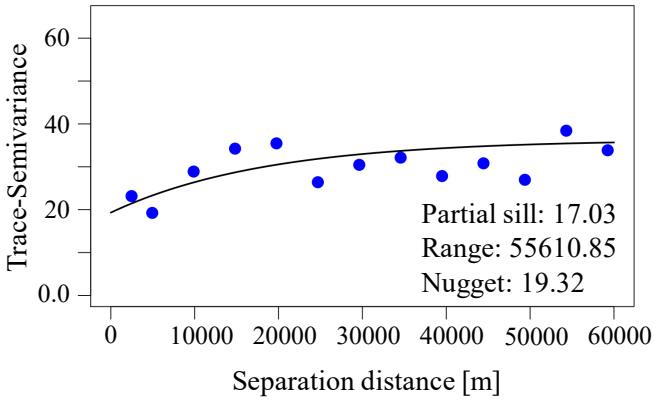

Figure 3. Sample trace-variogram estimated from the smoothed functional data for ammonium log-concentrations and interpreted model with estimated parameters.

An exponential model with nugget was fitted to the empirical variogram, estimated values of its parameters being included in Figure 3. One may notice the presence of a relevant nugget effect in the structure of spatial dependence, which provides an indication of possible spatial discontinuities in the field of NBL densities. Point Kriging was then performed across a regular grid of 2824 points (of side 983 m and 1048 m along the horizontal -West-East- and vertical -South-North- directions). Such a grid encompasses the full aquifer body domain, grid spacing being consistent with the spatial density of the available monitoring network and corresponding to a discretization of the variogram range (Figure 3) with about 50 points. Figure 4a depicts the resulting kriging-based predictions of PDFs of NBL of (log-transformed) ammonium concentrations. We note that, while point Kriging results do not depend on the cell size, the latter can be otherwise influential to the graphical representation associated with the color scale in Figure 4, which can nevertheless capture the overall spatial pattern of the quantities of interest. Cross-validation results (Appendix A) fully support the satisfactory performance of the prediction method.

Figures 4b and 4c illustrate the mean and standard deviation of the predicted NBL densities, respectively. The highest mean values are mostly located in the eastern portion of the domain, close to the coastal groundwater body, with moderate values of standard deviation. These results are consistent with the observation that raw concentration data collected from this area tend to exhibit large NH_4 values that persist over time (see also Figure 2), a finding which is possibly linked to ammonium being more soluble in saline environments as compared to freshwater bodies.

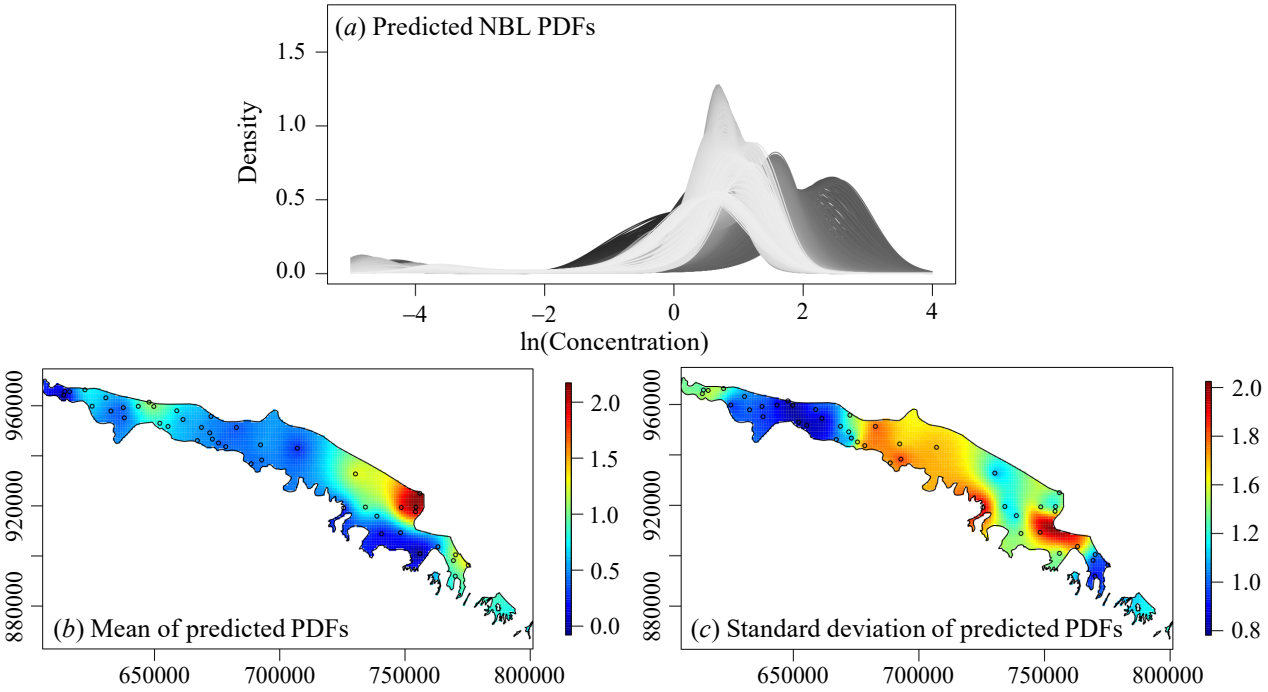

Figure 4. Kriging prediction of NBL densities for ammonium log-concentrations: (a) kriged/predicted densities; (b) mean values, and (c) standard deviation estimated from the kriged densities.

A sector characterized by low mean and high standard deviation values is visible in the south of this area. This result is consistent with the documented pattern associated with experimental data in this region, which are characterized by a temporal evolution displaying high concentration values within a collection of otherwise low values. The central portion of the domain is characterized by modest mean concentration values with high standard deviations. Low mean values and low to moderate values of standard deviation are found within the western area. It is noted that demarcation of zones linked to differing behaviors of the target chemical species is one

of the key advantages of the functional analysis approach we employ. Local high values of ammonium are consistent with the documented natural occurrence of paleo-peats (Amorosi et al., 1996; Cremonini et al., 2008) in sample cores collected at other locations across the area of interest, with an overall tendency of ammonium concentrations to increase with depth and with increasing thickness of the fine deposits that confine the aquifer. Further large scale sampling campaigns would be required for a detailed assessment of correspondences with specific local conditions.

Figure 5a depicts the predicted spatial variability of the 90% quantile of the NBL concentration. These results are complemented by Figure 5b, where we depict the spatial distribution of the probability of exceeding the reference NBL value of 4.6 mg/l, which was suggested by Molinari et al. (2012) as representative of the global chemical status of the system upon relying on the classical PS procedure, as proposed by Wendland et al. (2005) and described in Section 2.3.1. The stark variability displayed by the 90^{th} percentile across the domain documents the presence of sectors within which the target chemical species shows differing behavior and suggests the need for considering spatially variable local NBL values. Our results indicate that the probability of exceeding the reference NBL value of 4.6 mg/l is very low across most of the domain, high probability of exceedance being confined within a limited portion of the system.

We note that our results are in general agreement with the findings of Molinari et al. (2019), where areas where such probability was evaluated above 80% are slightly wider than in our findings, while being located in the same sector. We remark that the approach employed by these authors (*i*) is based solely on summary statistics and not on the entire PDFs and (*ii*) relies on a Gaussian assumption to represent (log-transformed) NBL concentrations. Additionally, it is noted that data associated with boreholes with less than 10 records (after PS) were excluded from our analysis to allow for PDF reconstruction and interpretation, while some of these were retained by Molinari et al. (2019). Finally, we highlight that our approach is fully compatible with the possibility of resorting to a multimodel analysis to comprise uncertainty about the choice of the functional format for the variogram model (see e.g., Molinari et al. (2019)). While this element can

be of interest, we focus here on the main innovative aspect of our study, which is related to the treatment of the data within the context of a functional geostatistical approach.

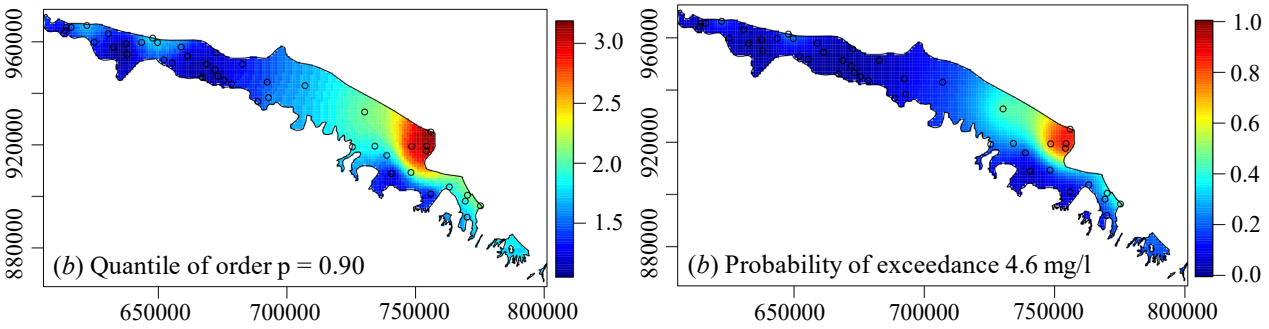

Figure 5. Spatial distributions of predicted (a) quantile of order 90% and (b) probability of exceedance of an ammonium concentration threshold of 4.6 mg/l.

The approach illustrated in Section 2.3.5 was then applied to the smoothed density data projected on the basis generated by the first $k = 8$ principal components (explaining 99.99% of the total variability) to generate a collection of random realizations of spatial distributions of NBL log-concentration values. The scores x_{s_1,k_1}, x_{s_2,k_2} were modeled as uncorrelated for $k_1 \neq k_2$ and $s_1 \neq s_2$ in the domain, as supported by visual inspection of cross-variograms (not shown). An exponential model was calibrated to the empirical variogram for each spatial field of scores. Conditional Gaussian simulations were performed to yield a Monte Carlo (MC) collection of 100 realizations. The practical implementation relies on the adoption of sequential Gaussian simulation (Abrahamsen and Benth, 2001) as implemented within the R package gstat (Pebesma, 2004), and setting a local neighborhood of 60 km to reduce computational burden. The collection of NBL distributions was then built from the MC ensemble of scores.

Figure 6 depicts a realization of the spatial field of NBL densities (Figure 6a), the spatial distributions of the 90% quantile (Figure 6b) and the probability of exceeding the threshold value of 4.6 mg/l (Figure 6c). Similar to what we observed in Figure 5, the overall spatial pattern in Figures 6b, c is generally consistent with the results presented by Molinari et al. (2019) (see their Figure 2) and reinforces the concept that assigning a unique NBL value for a given chemical species to a

large scale groundwater body can conceal the possibility of identifying regions with high (or low) geogenic contribution. These could in turn be ascribed to low (or high) anthropogenic activity, thus potentially biasing expectations about results of groundwater protection measures. We recall that Molinari et al. (2019) (*a*) rely on the stringent assumption that (log)concentrations can be described as a Gaussian model, and (*b*) parametrize the latter on the basis of kriging results relying solely on summary statistics evaluated from the available data. Rather, we are not limited by any assumption about the specific functional format of probability densities, which are entirely data-driven and are the object of the geostatistical analysis. As such, the tools and implementation workflow we propose is conducive to evaluations of the spatially heterogeneous field of NBL values in a probabilistic context upon maximizing the use of the amount of information embedded in the available data. This is seen as a critical element of a modern decision-making approach grounded on a firm environmental risk assessment practice. Future integration of these findings with other types of (hydro)geological and geochemical information can then yield a complete picture of the natural signature of the system analyzed.

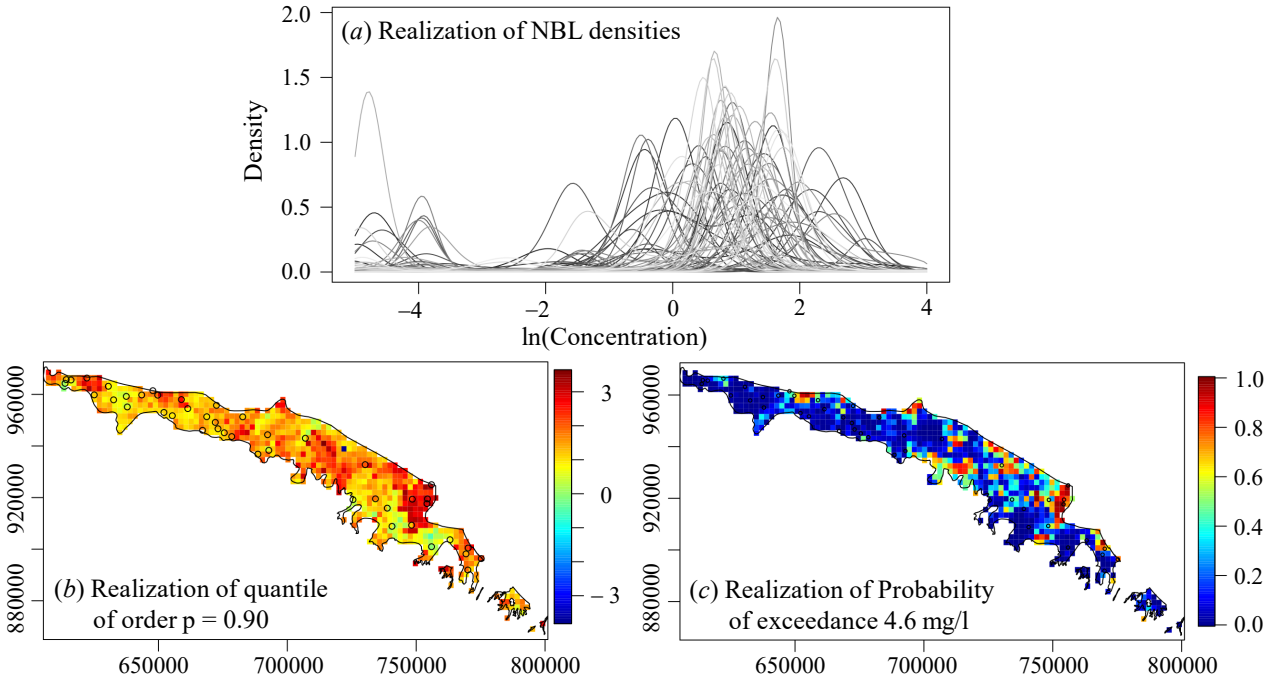

Figure 6. Example of a realization obtained from the (conditional) stochastic simulation of NBL distributions of ammonium log-concentrations. (a) Simulated NBL densities and corresponding spatial distributions, (b) 90% quantiles, (c) probability of exceeding a threshold value of 4.6 mg/l.

3.2. Arsenic

A total of 1096 data collected at 43 monitoring station were available for arsenic after PS (see Section 2.1), with a number of observations per sampling point ranging between 11 to 38 (with an average of about 25). Estimation of the PDF of the NBL concentrations is performed at each borehole location consistently with the approach exemplified in Section 3.1. The resulting smoothed data are depicted in Figure 7.

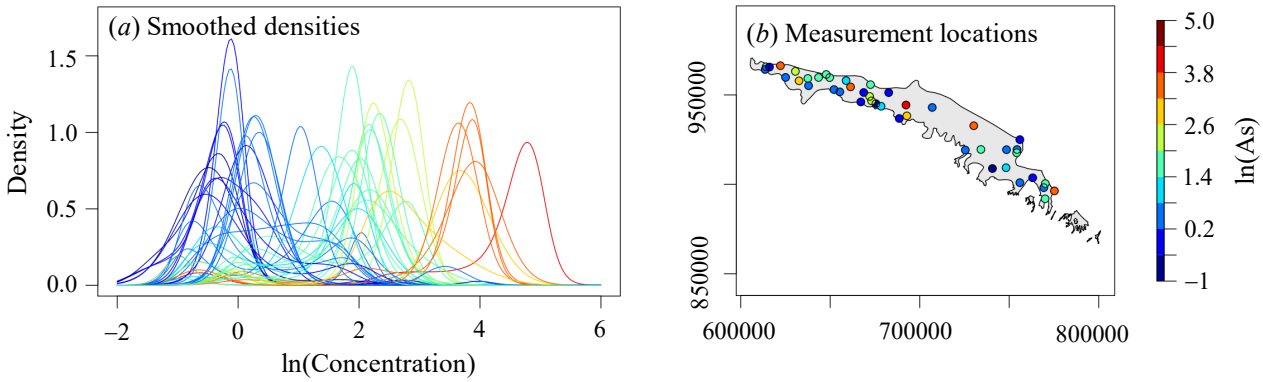

Figure 7. Smoothed data for arsenic log-concentrations (a), and corresponding spatial locations in the investigated aquifer system (b). Colors are assigned according to the value of the mean related to the corresponding smoothed density.

Figure 7 suggests a significant spatially heterogeneous behavior. The highest mean values are scattered across the whole domain, suggesting that these could be associated with local conditions. These types of results are consistent with the behavior of arsenic, that is typically documented to display a remarkably high degree of spatial variability within a given groundwater body (e.g., Duan et al., 2017; Pi et al., 2018; Smith et al., 2003; Liang et al., 2017, 2018, 2019).

The sample trace-variogram associated with the available densities is depicted in Figure 8, its pattern supporting a global stationarity assumption. An exponential model with nugget was calibrated to the empirical variogram, its estimated parameters being listed in Figure 8. The contribution of the nugget to the total variance is equal to 15%, suggesting the occurrence of variability between sample pairs separated by short distance.

The available smoothed densities were then estimated through Kriging at the same set of unsampled locations considered in the ammonium case, grid spacing corresponding to a discretization of the variogram range (Figure 8) with about 10 points. Cross-validation results (Appendix A) fully support the satisfactory performance of the approach.

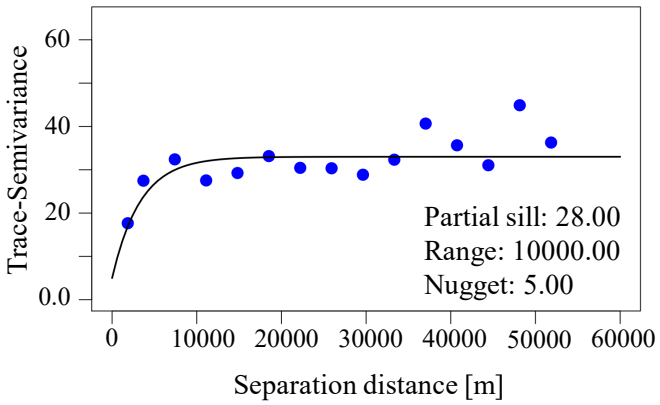

Figure 8. Sample trace-variogram estimated from the smoothed functional data for arsenic log-concentrations and interpreted model with estimated parameters.

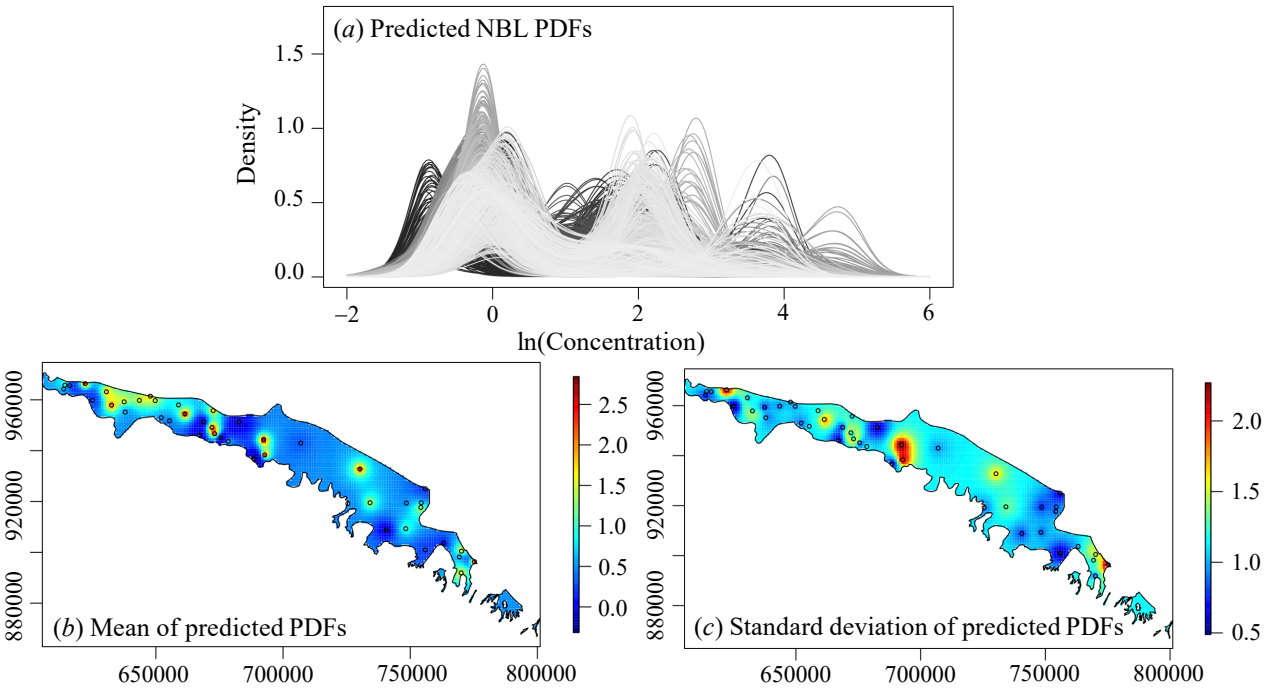

Figure 9. Kriging prediction of NBL densities for arsenic log-concentrations: (a) kriged/predicted density functions; (b) spatial distribution of mean values, and (c) standard deviation estimated from the kriged densities.

Figure 9a depicts the predicted (i.e., based on functional Kriging results) PDFs of NBL log-concentrations of arsenic. Figures 9b and 9c depict the estimates of mean value and standard deviation of NBL densities, respectively. Moderate to high mean values are mostly located in the north-western and central portions of the domain. The associated standard deviation varies from moderate to high values. Areas characterized by high values of the mean value of predicted PDFs appear to be localized around some measurement stations, rather than being spread across extended sectors of the domain. This finding is also consistent with possible occurrences of lateral variations of arsenic concentrations, similar to other documented studies across several regions worldwide.

Figure 10a depicts the spatially heterogeneous distribution of the predicted 90% quantile of the NBL As log-concentrations. To complement these results, Figure 10b shows the probability of exceeding the reference NBL value of 33 µg/l, evaluated by Molinari et al. (2012) as representative of the global chemical status of the system through the classical PS procedure (Wendland et al., 2005). We found that the probability of exceeding such a threshold value is very modest throughout the system, with the exception of some localized spots where it attains moderate values. This has a clear consequence on the assessment of the chemical status of the system, which would have been (deterministically) classified as requiring attention on the basis of such a performance metric.

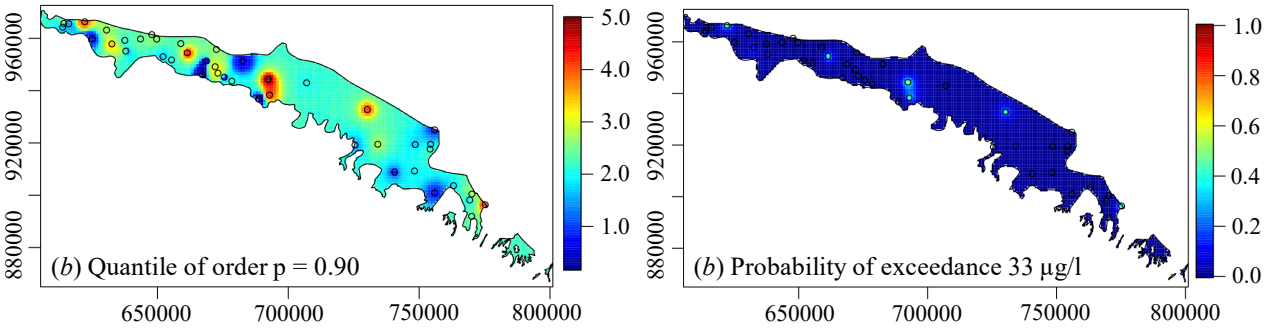

Figure 10. Spatial distribution of predicted (a) 90% quantile and (b) probability of exceedance of an arsenic concentration threshold of 33 µg/l.

We note that Molinari et al. (2019) could not provide spatial maps of exceedance probabilities, because their analysis, grounded solely on summary quantities, resulted in a pure nugget semivariogram. Our results suggest that considering a functional analysis approach might

enable one to observe the emergence of some degree of spatial correlation when the complete density associated with observations is embedded in the methodology.

Similar to the case of ammonium, we applied the stochastic simulation approach described in Section 2.3.5 to the smoothed density data projected on the basis generated by the first $k = 8$ principal components (explaning 99.99% of the total variability). MC realizations employed a local neighborhood of 60 km being set to alleviate computational time. Figure 11 depicts a selected realization of the spatial field of NBL densities (Figure 11a), the corresponding spatial distributions of 90% quantiles (Figure 11b), and the probability of exceeding the threshold value of 33 µg/l (Figure 11c). The occurrence of localized spots associated with significant probability of high natural arsenic concentrations are consistent with the documented presence at some depths in the aquifer system of sediments whose composition includes a vegetal-rich fraction (see, e.g., Molinari et al., 2013, 2014). These types of solid matrices are prone to potentially adsorb significant arsenic amounts that can then be mobilized by variations of redox conditions (see, e.g., Molinari et al., 2013, 2014, 2015). A detailed analysis to evaluate possible relationships and consistency with local conditions would require additional large scale sampling campaigns which can be subject of future studies.

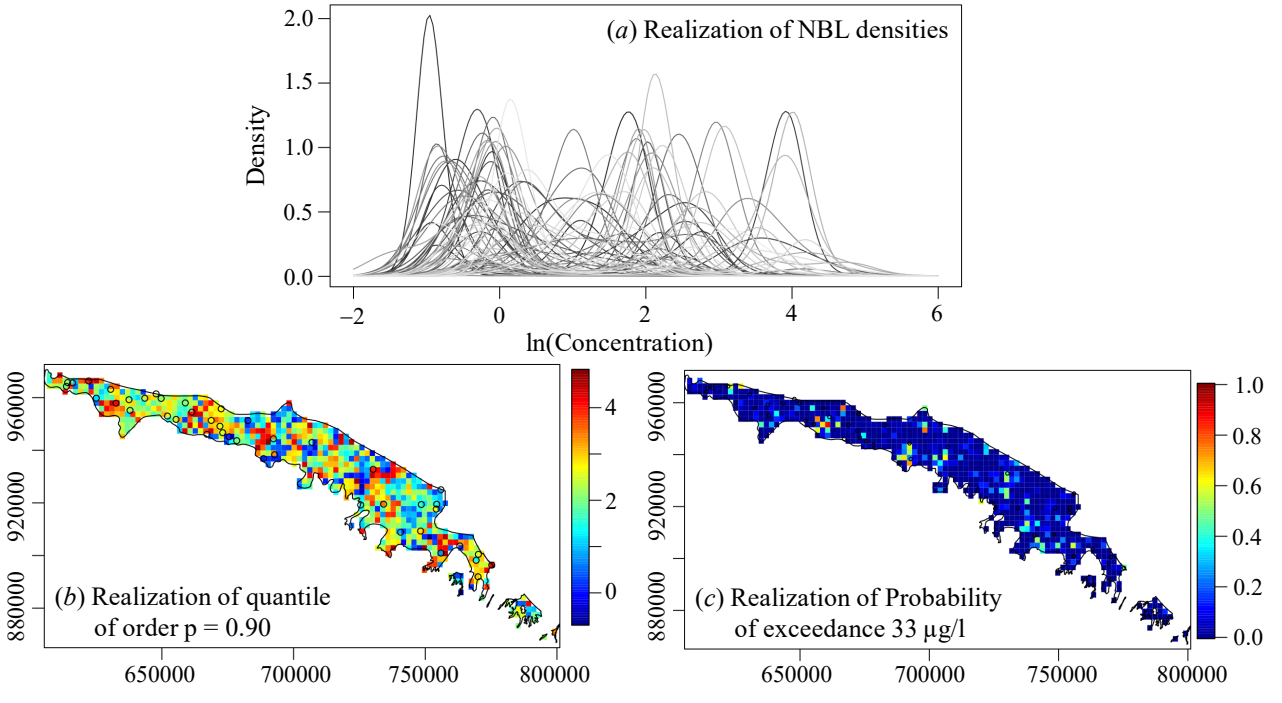

Figure 11. Example of a realization obtained from the (conditional) stochastic simulation of NBL distributions of arsenic. (a) Simulated NBL densities and corresponding spatial distributions of (b) 90% quantiles, and (c) probability of exceeding the threshold value of 33 μg/l.

4. Conclusions

We propose and apply a theoretical framework and the ensuing operational workflow to obtain a rigorous (probabilistic) assessment of Natural Background Levels (NBL) of concentrations of target chemical species in large-scale groundwater bodies, which are usually characterized by a high degree of heterogeneity of sedimentological and hydrogeochemical conditions. Our approach enables one to fully consider the richness of information embedded in the available historical records of routinely monitored concentrations which are then typically employed (e.g., by Environmental Agencies) to assess the chemical status of a groundwater body. On these bases, we suggest a change of perspective in the way one should consider evaluating NBL concentrations in a modern probabilistic risk assessment context. Rather than focusing on selected (statistical) moments or percentiles (i.e., summary statistics) evaluated on the basis of sample probability distributions of concentrations at individual boreholes, we associate with each monitoring station the entire distribution of NBL concentrations. The latter is represented through its (estimated) density function, which we model as a random point in a Bayesian Hilbert space and then analyze in the context of Object Oriented Data Analysis. The merits of the approach are exemplified through an application targeting the evaluation of the main characteristics of the spatial variability of the NBLs of two selected chemical species (ammonium and arsenic) within a large scale groundwater body in Northern Italy.

Our study leads to the following major conclusions.

1. The approach enables one to identify local trends within a given groundwater body, as quantified in terms of spatial heterogeneity of NBL concentrations, in a probabilistic context, without being limited to relying solely on selected quantiles of the distribution of concentrations extracted from historical records. As such, it is possible to demarcate sectors

where distinct NBL spatial patterns emerge from an average system behavior, to be then integrated within a decision-making activity.

2. The approach is fully consistent with modern requirements of tailoring the objective of environmental actions to spatially varying conditions. This forms the platform to set appropriate and cost-effective remediation goals and actions for deteriorated groundwater bodies which account for the complete set of information embedded in the historical records. Relying on rigorously assessed spatial distributions of probabilities of exceeding given NBL concentration thresholds hampers the risk of assigning exceedingly high values of natural background concentrations to areas subject to anthropogenic activities or otherwise setting very low background levels within regions where the geogenic contribution can be significant. Lack of consideration of these elements could lead to setting unrealistic remediation goals.
3. Having the ability to generate multiple conditional spatial realizations of NBL densities enables a complete uncertainty quantification (see our exemplary results in Section 3) which would be otherwise impossible with standard methods of analysis currently adopted in practical applications targeting large scale groundwater bodies. These elements are markedly relevant in such systems, whose hydrogeologic, lithologic, and geochemical characteristics can be associated with large spatial heterogeneity.

Key values of the study are methodological as well as operational. From a methodological standpoint, the workflow we propose includes elements of innovation which go beyond limitations of other typically used approaches, including the possibility of effectively using the full information content embedded in data which are routinely monitored by local authorities and public environmental agencies. From an operational standpoint, it provides an appraisal of the probability that a given threshold value of concentration of geogenic origin can be exceeded in the exemplary areas considered. The ability to provide a robust and data-driven quantification of probability of exceedance provides an important element of flexibility in decision-making under uncertainty. The

543 nature of the approach allows accounting for specific local needs, as viewed in the broad regional
544 context, as well as the possibility of updating the results of the analysis as data become available.
545 As such, it enables one to structure corrective actions according to levels of priorities related to
546 target concentration thresholds and associated probability distributions linked to specific areas,
547 which might be characterized by distinct local requirements. In this sense, our results can provide a
548 support to identify localized areas where detailed hydrogeological studies can be promoted with the
549 aim, e.g., to constrain uncertainty associated with predicted NBL values and associated probability
550 of exceedance.
551

Appendix A

The performance of the proposed approach is assessed through a leave-one-out cross-validation (LOO CV) analysis. Here, for each site s_i in D, the PDF of the NBL PDF X_{s_i} is left out of the sample and a training set built upon all of the other NBL PDFs, $\{X_{s_j}, j \neq i\}$, is considered for calibration of the geostatistical model, following the same steps and parameter settings as in Section 3. Kriging is then used to predict the left-out NBL PDF X_{s_i}, yielding a prediction $X_{s_i}^{*(-i)}$. The prediction error for each site is evaluated through the sum of squared errors (SSE) as

$$\mathrm{SSE}(X_{s_i}) = d_{B^2}^2\left(X_{s_i}, X_{s_i}^{*(-i)}\right) = \frac{1}{2(b-a)}\int_a^b\int_a^b \ln\left(\frac{X_{s_i}(t)X_{s_i}^{*(-i)}(s)}{X_{s_i}(s)X_{s_i}^{*(-i)}(t)}\right) dtds. \quad \text{(A1)}$$

Table A1 lists the summary statistics of SSE, as assessed via LOO CV for ammonium (first row) and arsenic (second row). It is noted that the LOO CV analyses for these chemical species are performed separately. Overall, the order of magnitude of the errors is fully consistent with the estimated sills of the trace-variograms (estimated sills: 36.35 and 33.00 for ammonium and arsenic, respectively).

Chemical Species	Min	Q1	Median	Mean	Q3	Max
Ammonium	8.81	18.16	26.58	29.97	40.01	109.08
Arsenic	9.84	19.91	26.96	35.43	36.32	134.37

Table A1: Summary statistics for SSE (A1).

The LOO CV analysis is additionally used to evaluate the ability of our conditional simulation theoretical approach and operational workflow to represent prediction uncertainty. As an example, Figure A1 depicts the results obtained at two locations (denoted as FC17−01 and RE17−03) for ammonium (top panels) and arsenic (bottom panels). Predicted NBL PDFs at these locations are depicted with dashed black curves, whereas grey curves correspond to the $B = 100$ conditional simulations at the site. The observed PDFs are represented as thick black curves. Visual inspection of Figure A1 suggests that conditional simulations well represent the uncertainty associated with the

predictions for both chemical species. For instance, one can observe that, even as the kriging error for arsenic at location RE17-03 appears to be quite high, the conditional simulations at the site suggest that a high uncertainty is associated with the prediction. Note that here, the test NBL PDF is well captured by the simulated collection of realizations.

To quantitatively assess the performance in terms of uncertainty quantification, we then compute the distance between the test curve and the ensemble of Monte Carlo simulations as

$$\mathrm{SSE_{sim}}\left(\mathrm{X_{s_i}}\right) = \min\left\{\mathrm{d_{B^2}^2}\left(\mathrm{X_{s_i}}, \mathrm{X_{s_i}^{b(-i)}}\right), \mathrm{b} = 1, \ldots \mathrm{B}\right\} \quad \text{(A2)}$$

where $\mathrm{X_{s_i}^{b(-i)}}$ denotes the b-th conditional simulation when the i-th observation is left out of the sample. In practice, the smaller $\mathrm{SSE_{sim}}\left(\mathrm{X_{s_i}}\right)$, the closer the ensemble is to the test observation $\mathrm{X_{s_i}}$. For instance, values of $\mathrm{SSE_{sim}}\left(\mathrm{X_{s_i}}\right)$ for ammonium at locations FC17-01 and RE17-03 are 5.96 and 7.56, respectively, their counterparts corresponding to arsenic being 16.46 and 10.28, respectively. Table 2 lists the summary statistics associated with $\mathrm{SSE_{sim}}$ for both chemical species. One can note that the ensemble is typically quite close to the test observation, with an average $\mathrm{SSE_{sim}}$ of 10.67 and 9.02 for ammonium and arsenic, respectively.

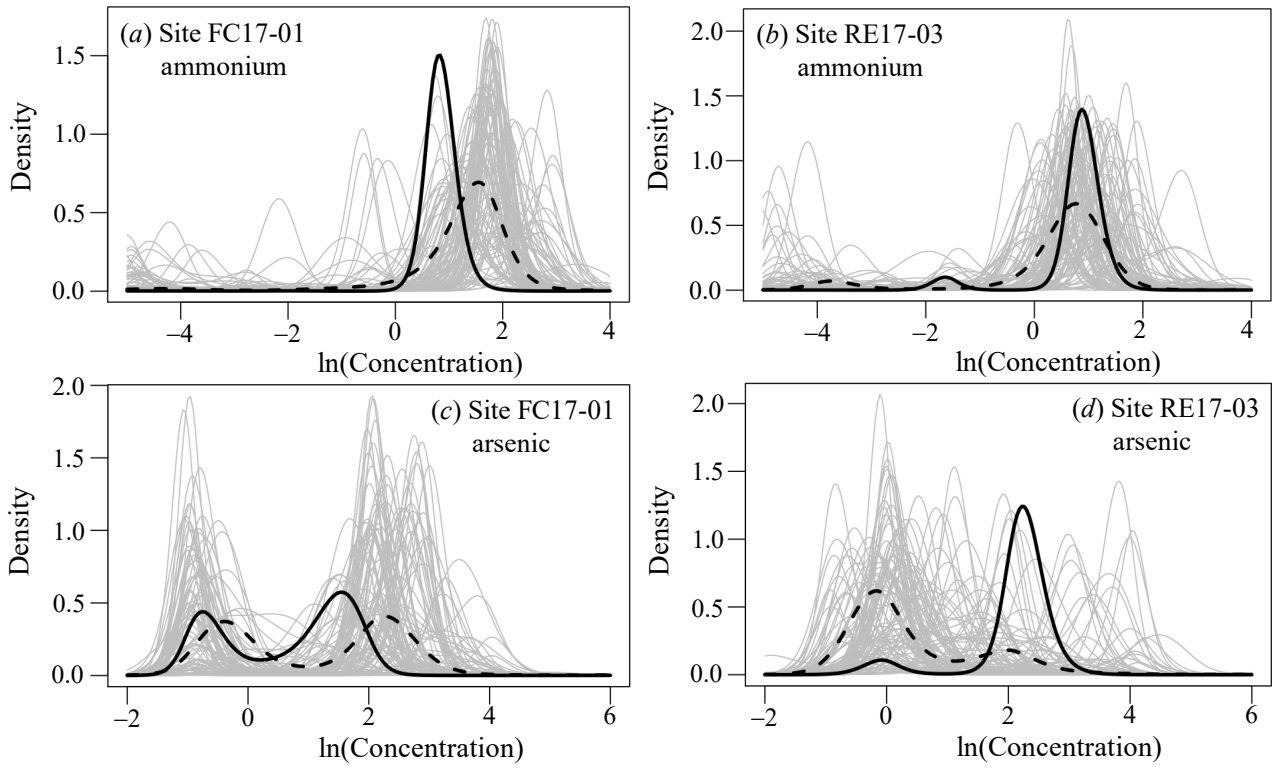

588 *Figure A1. Leave-one-out cross-validation results at sites FC17-01 and RE17-03. Dashed black*
589 *curves correspond to predicted NBL PDFs, whereas grey curves correspond to the* $B = 100$
590 *conditional simulations at the site; observed PDFs are represented as thick black curves.*
591

Chemical Species	Min	Q1	Median	Mean	Q3	Max
Ammonium	2.30	5.70	7.88	10.67	13.15	41.92
Arsenic	1.05	5.31	7.14	9.023	10.56	30.38

592 *Table A2: Summary statistics for* $\mathrm{SSE}_{\mathrm{sim}}$ *(A2).*

593 **References**

594 Aitchison, J., 1986. The statistical analysis of compositional data. Chapmann and Hall, New York.

595 Abrahamsen, P., Benth, F., 2001. Kriging with inequality constraints. Math. Geol. 33(6), 719-744.
596 https://doi.org/10.1023/A:1011078716252.

597 Amorosi, A., Farina, M., Severi, P., Preti, D., Caporale, L., Di Dio, G., 1996. Genetically related
598 alluvial deposits across active fault zones: an example of alluvial fan-terrace correlation
599 from the upper Quaternary of the southern Po Basin, Italy. Sediment. Geol. 102, 275-295.
600 https://doi.org/10.1016/0037-0738(95)00074-7.

601 Bianchi Janetti, E., Guadagnini, L., Riva, M., Guadagnini, A., 2019. Global sensitivity analysis of
602 multiple conceptual models with uncertain parameters driving groundwater flow in a
603 regional-scale sedimentary aquifer. J. Hydrol. 574, 544-556.
604 https://doi.org/10.1016/j.jhydrol.2019.04.035

605 BRIDGE - Background cRiteria for the IDentification of Groundwater thrEsholds 2007. http://nfp-
606 at.eionet.europa.eu/irc/eionet-circle/bridge/info/data/en/index.htm (accessed 21 February
607 2020); or https://cordis.europa.eu/result/rcn/51965_en.html (accessed 21 February 2020).

608 Chilès, J.P., Delfiner, P., 1999. Geostatistics: Modeling spatial uncertainty, John Wiley & Sons,
609 New York.

610 Cremonini, S., Etiope, G., Italiano, F., Martinelli, G., 2008. Evidence of possible enhanced peat
611 burning by deep-origin methane in the Po River delta Plain (Italy). J. Geol. 116, 401-413.
612 https://doi.org/10.1086/588835.
613 Dalla Libera, N., Fabbri, P., Mason, L., Piccinini, L., Pola, M., 2017. Geostatistics as a tool to
614 improve the natural background level definition: an application in groundwater. Sci. Total
615 Environ. 598, 330-340. https://doi.org/10.1016/j.scitotenv.2017.04.018.
616 Decreto Legislativo n. 30 del 16 marzo 2009 (Legislation Decree n. 30, 16 March, 2009).
617 Application of the Directive 2006/118/CE, related to the protection of groundwater
618 resources from pollution and deterioration (Attuazione della direttiva 2006/118/CE, relativa
619 alla protezione delle acque sotterranee dall'inquinamento e dal deterioramento). Gazzetta
620 Ufficiale n. 79 of 4 April 2009 (in Italian).
621 Directive 2000/60/EC - Water Framework Directive (WFD). Directive of the European Parliament
622 and of the Council of 23 October 2000 establishing a framework for Community action in
623 the field of water policy, OJ L327, 22 Dec 2000, 1-73.
624 Directive 2006/118/EC, GroundWater Daughter Directive (GWDD). Directive of the European
625 Parliament and of the Council of 12 December 2006 on the protection of groundwater
626 against pollution and deterioration, OJ L372, 27 Dec 2006, 19-31.
627 Directive 2014/80/EU amending Annex II to Directive 2006/118/EC of the European Parliament
628 and of the Council on the Protection of Groundwater Against Pollution and Deterioration,
629 OJ L182, 21 June 2014, 52-55.
630 Duan, Y., Gan, Y., Wang, Y., Liu, C., Yu, K., Deng, Y., Zhao, K., Dong, C., 2017. Arsenic
631 speciation in aquifer sediment under varying groundwater regime and redox conditions at
632 Jianghan Plain of Central China. Sci. Total Environ. 607-608, 992-1000.
633 https://doi.org/10.1016/j.scitotenv.2017.07.011.
634 Ducci, D., Condesso de Melo, M.T., Preziosi, E., Sellerino, M., Parrone, D., Ribeiro, L., 2016.
635 Combining natural background levels (NBLs) assessment with indicator kriging analysis to

636 improve groundwater quality data interpretation and management. Sci. Total Environ. 569-
637 570, 569-584. https://doi.org/10.1016/j.scitotenv.2016.06.184.
638 Edmunds, W.M., Shand, P., Hart, P., Ward, R.S., 2003. The natural (baseline) quality of
639 groundwater: a UK pilot study. Sci. Total Environ. 310 (1-3), 25-35.
640 https://doi.org/10.1016/S0048-9697(02)00620-4.
641 Egozcue, J. J., Díaz-Barrero, J.L., Pawlowsky-Glahn, V., 2006. Hilbert space of probability density
642 functions based on Aitchison geometry. Acta Math. Sin. Engl. Ser. 22(4), 1175- 1182.
643 https://doi.org/10.1007/s10114-005-0678-2.
644 Farina, M., Marcaccio, M., Zavatti, A., 2014. Experiences and perspectives to monitoring of
645 groundwater resources: the contribution of Emilia Romagna (Esperienze e prospettive nel
646 monitoraggio delle acque sotterranee: il contributo dell'Emilia-Romagna), Pitagora Editrice,
647 Bologna (in Italian).
648 Hinsby, K., Condesso de Melo, M.T., 2006. Application and evaluation of a proposed methodology
649 for derivation of groundwater threshold values-a case study summary report. In Deliverable
650 D22 of the EU project ‘‘BRIDGE’’ 2006. http://nfp-at.eionet.europa.eu/Public/irc/eionet-
651 circle/bridge/library?l=/deliverables/d22_final_reppdf/_EN_1.0_&a=d. (accessed 21
652 February 2020).
653 Hinsby, K., Condesso de Melo, M.T., Dahl, M., 2008. European case studies supporting the
654 derivation of natural background levels and groundwater threshold values for the protection
655 of dependent ecosystems and human health. Sci. Total Environ. 401(1-3), 1-20.
656 https://doi.org/10.1016/j.scitotenv.2008.03.018.
657 Hron, K., Menafoglio, A., Templ, M., Hruzova, K., Filzmoser, P., 2016. Simplicial principal
658 component analysis for density functions in Bayes spaces. Comput. Stat. Data An. 94, 330–
659 350. https://doi.org/10.1016/j.csda.2015.07.007.

660 Kim, K.H., Yun, S.T., Kim, H.K., Kim, J.W., 2015. Determination of natural backgrounds and
661 thresholds of nitrate in South Korean groundwater using model-based statistical approaches.
662 J. Geochem. Explor. 148, 196-205. https://doi.org/10.1016/j.gexplo.2014.10.001.
663 Kim, H.R., Kim, K.H., Yu, S., Moniruzzaman, M., Hwang, S.I., Lee, G.T., Yun, S.T., 2019. Better
664 assessment of the distribution of As and Pb in soils in a former smelting area, using ordinary
665 co-kriging and sequential Gaussian co-simulation of portable X-ray fluorescence (PXRF)
666 and ICP-AES data. Geoderma 341, 26-38. https://doi.org/10.1016/j.geoderma.2019.01.031.
667 Li, P., Qian, H., Howard, K.W.F., Wu, J., Lyu, X., 2014. Anthropogenic pollution and variability of
668 manganese in alluvial sediments of the Yellow River, Ningxia, northwest China. Environ.
669 Monit. Assess. 186(3), 1385-1398. https://doi.org/10.1007/s10661-013-3461-3.
670 Liang, C.P., Hsu, W.S., Chien, Y.C., Wang, S.W., Chen, J.S., 2019. The combined use of
671 groundwater quality, drawdown index and land use to establish a multi-purpose groundwater
672 utilization plan. Water Resour. Manag. 33, 4231-4247, https://doi.org/10.1007/s11269-019-
673 02360-2.
674 Liang, C.P., Chen, J.S., Chien, Y.C., Jang, C.S., Chen, C.F., 2018. Spatial analysis of the risk to
675 human health from exposure to arsenic contaminated groundwater: a kriging approach. Sci.
676 Total Environ. 627, 1048-1057. doi: 10.1016/j.scitotenv.2018.01.294.
677 Liang, C.P., Chien, Y.C., Jang, C.S., Chen, C.F., Chen, J.S., 2017. Spatial analysis of human health
678 risk due to arsenic exposure through drinking groundwater in Taiwan's Pingtung Plain. Int.
679 J. Environ. Res. Public Health, 14, 81. doi:10.3390/ijerph14010081.
680 Machalová, J., Hron, K., Monti, G.S., 2016. Preprocessing of centred logratio transformed density
681 functions using smoothing splines. J. Appl. Stat. 43(8), 1419-1435.
682 https://doi.org/10.1080/02664763.2015.1103706.
683 Marron, J.S., Alonso, A.M., 2014. Overview of object oriented data analysis. Biometrical J. 56(5),
684 732-753. https://doi.org/10.1002/bimj.201300072.

685 Menafoglio, A., Secchi, P., Dalla Rosa, M., 2013. A Universal Kriging predictor for spatially
686 dependent functional data of a Hilbert Space. Electron. J. Statist. 7, 2209–2240.
687 https://doi.org/10.1214/13-EJS843.
688 Menafoglio, A., Guadagnini, A., Secchi, P., 2014. A Kriging approach based on Aitchison
689 geometry for the characterization of particle-size curves in heterogeneous aquifers. Stoch.
690 Environ. Res. Risk Assess. 28(7), 1835-1851. https://doi.org/10.1007/s00477-014-0849-8.
691 Menafoglio, A., Secchi, P., Guadagnini, A., 2016a. A Class-Kriging predictor for Functional
692 Compositions with application to particle-size curves in heterogeneous aquifers. Math.
693 Geosci. 48(4), 463-485. https://doi.org/10.1007/s11004-015-9625-7.
694 Menafoglio, A., Guadagnini, A., Secchi, P., 2016b. Stochastic Simulation of soil particle-size
695 curves in heterogeneous aquifer systems through a bayes space approach. Water Resour.
696 Res. 52, 5708–5726. https://doi.org/10.1002/2015WR018369.
697 Menafoglio, A., Secchi, P., 2017. Statistical analysis of complex and spatially dependent data: A
698 review of object oriented spatial statistics. Eur. J. Oper. Res. 258(2), 401-410.
699 https://doi.org/10.1016/j.ejor.2016.09.061.
700 Molinari, A., Guadagnini, L., Marcaccio, M., Guadagnini, A., 2012. Natural background levels and
701 threshold values of chemical species in three large-scale groundwater bodies in Northern
702 Italy. Sci. Total Environ. 425, 9-19. https://doi.org/10.1016/j.scitotenv.2012.03.015.
703 Molinari, A., Guadagnini, L., Marcaccio, M., Straface, S., Sanchez-Vila, X., Guadagnini, A., 2013.
704 Arsenic release from deep natural solid matrices under experimentally controlled redox
705 conditions. Sci. Total Environ. 444, 231-240.
706 https://doi.org/10.1016/j.scitotenv.2012.11.093.
707 Molinari, A., Ayora, C., Marcaccio, M., Guadagnini, L., Sanchez-Vila, X., Guadagnini, A. 2014.
708 Geochemical modeling of arsenic release from a deep natural solid matrix under alternated
709 redox conditions. Environ. Sci. Pollut. Res. 21, 1628-1637. https://doi.org/10.1007/s11356-
710 013-2054-6.

711 Molinari, A., Guadagnini, L., Marcaccio, M., Guadagnini, A., 2015. Arsenic fractioning in natural
712 solid matrices sampled in a deep groundwater body. Geoderma 247-248, 88-96.
713 https://doi.org/10.1016/j.geoderma.2015.02.011.
714 Molinari, A., Guadagnini, L., Marcaccio, M., Guadagnini, A., 2019. Geostatistical multimodel
715 approach for the assessment of the spatial distribution of natural background concentrations
716 in large-scale groundwater bodies. Water. Res. 149, 522-532.
717 https://doi.org/10.1016/j.watres.2018.09.049.
718 Panno, S.V., Kelly, W.R., Martinsek, A.T., Hackley, K.C., 2006. Estimating background and
719 threshold nitrate concentrations using probability graphs. Groundwater 44(5), 697-709.
720 https://doi.org/10.1111/j.1745-6584.2006.00240.x
721 Pebesma, E. J., 2004. Multivariable geostatistics in S: the gstat package. Computers & Geosciences
722 30, 683-691. https://doi.org/10.1016/j.cageo.2004.03.012.
723 Perulero Serrano, R., Guadagnini, L., Riva, M., Giudici, M., Guadagnini, A., 2014. Impact of two
724 geostatistical hydro-facies simulation strategies on head statistics under non-uniform
725 groundwater flow. J. Hydrology 508, 343-355.
726 https://doi.org/10.1016/j.jhydrol.2013.11.009.
727 Pi, K., Wang, Y., Postma, D., Ma, T., Su, C., Xie, X., 2018. Vertical variability of arsenic
728 concentrations under the control of iron-sulfur-arsenic interactions in reducing aquifer
729 systems. J. Hydrol. 561, 200-210. https://doi.org/10.1016/j.jhydrol.2018.03.049.
730 Redman, A.D., Macalady, D. L., Ahmann, D., 2002. Natural organic matter affects arsenic
731 speciation and sorption onto hematite. Environ. Sci. Technol. 36, 2889-2896.
732 https://doi.org/10.1021/es0112801.
733 Regione Emilia-Romagna, 2010. Council Decree (Delibera di Giunta) n. 350 of 8/02/2010,
734 Approval of the activities of the Emilia-Romagna Region related to the implementation of
735 Directive 2000/60/CE aiming at the design and adoption of the Management Plans of the
736 hydrographic districs Padano, Appennino settentrionale and Appennino centrale

737 (Approvazione delle attività della Regione Emilia-Romagna riguardanti l'implementazione
738 della Direttiva 2000/60/CE ai fini della redazione ed adozione dei Piani di Gestione dei
739 Distretti idrografici Padano, Appennino settentrionale e Appennino centrale).
740 http://ambiente.regione.emilia-romagna.it/acque/temi/piani%20di%20gestione (In Italian,
741 accessed 21 February 2020).
742 Regione Emilia-Romagna, ENI-AGIP, 1998. Riserve idriche sotterranee della Regione Emilia-
743 Romagna. S.EL.CA, Firenze.
744 Reimann, C., Garrett, R.G., 2005. Geochemical background: concept and reality. Sci. Total
745 Environ. 350, 12-27. https://doi.org/10.1016/j.scitotenv.2005.01.047.
746 Ricci Lucchi, F., 1984. Flysh, molassa, clastic deposits: traditional and innovative approaches to the
747 analysis of north Apeninic basins (Flysch, molassa, cunei clastici: tradizione e nuovi
748 approcci nell'analisi dei bacini orogenici dell'Appennino settentrionale). Cento Anni di
749 Geologia Italiana. Volume Giubilare 1° centenario Soc. Geol. Ital., 279-295 (in Italian).
750 Short, M., Guadagnini, L., Guadagnini, A., Tartakovsky, D. M., Higdon, D., 2010. Predicting
751 vertical connectivity within an aquifer system. Bayesian Analysis 5(3), 557-582.
752 https://doi.org/10.1214/10-BA522.
753 Smith, J.V.S, Jankowski, J., Sammut, J., 2003. Vertical distribution of As (III) and As (V) in a
754 coastal sandy aquifer: Factors controlling the concentration and speciation of arsenic in the
755 Stuarts Point groundwater system, northern New South Wales. Australia. Appl. Geochem.
756 18(9), 1479-1496. https://doi.org/10.1016/S0883-2927(03)00063-5.
757 Urresti-Estala, B., Carrasco-Cantos, F., Vadillo-Pérez, I., Jiménez-Gavilán, P., 2013. Determination
758 of background levels on water quality of groundwater bodies: A methodological proposal
759 applied to a Mediterranean river basin (Guadalhorce River, Málaga, southern Spain). J.
760 Environ. Manage. 117, 121-130. https://doi.org/10.1016/j.jenvman.2012.11.042.
761 Van den Boogaart, K. G., Egozcue, J.J., Pawlowsky-Glahn, V., 2014. Bayes Hilbert spaces. Aus.
762 N.Z. J. Stat. 56, 171-194. https://doi.org/10.1111/anzs.12074.

763 Walter, T., 2008. Determining natural background values with probability plots. EU Groundwater
764 Policy Developments Conference, UNESCO, Paris, France, 13-15 Nov 2008.
765 https://orbi.uliege.be/bitstream/2268/76101/1/actes_colloques_cfhaih_nov08.pdf (accessed
766 21 February 2020).
767 Wendland, F., Hannappel, S., Kunkel, R., Schenk, R., Voigt, H.J., Wolter, R., 2005. A procedure to
768 define natural groundwater conditions of groundwater bodies in Germany. Water Sci.
769 Technol. 51(3-4), 249-257. https://doi.org/10.2166/wst.2005.0598.
770 Winter, C.L., Tartakovsky, D.M., Guadagnini, A., 2003. Moment differential equations for flow in
771 highly heterogeneous porous media. Surv. Geophys. 24 (1), 81-106.
772 https://doi.org/10.1023/A:1022277418570.
773